ISSN No:-2456-2165

Nano Cellulose Particles from *Pandanus Utilis* and *Sansevieria Trifasciata* Significantly but Differently Improve the Tensile and Flexural Strength of Polyester Composites

Bookal Rohan Yashveer
Faculty of Engineering
UoM, Mauritius

Abstract:- Nano cellulose from plant fibres were selected as reinforcement. Sansevieria Trifasciata and Pandanus Utilis were selected as the source of the biomass. Polyester resin was selected as the matrix. The investigation involved the variables type of CNC and Wt. % of CNC in the matrix. Full factorial design of experiment was carried out. Composites was manufactured under vacuum and tensile and flexural test were performed as per ASTM standards. The maximum tensile and flexural strength were noted at 5 Wt.% of CNC, the mechanical strength of S.T CNC reinforced composite was always higher than that of P.U CNC one. A general increase in strength was noted as wt. % of CNC increased for both biomass.

Keywords:- *Nano cellulose; Pandanus Utilis; Sansevieria Trifasciata; composite; tensile strength; flexural strength.*

I. INTRODUCTION

Mauritius being part of the SIDS countries, is constantly on forefront of sustainable development challenges. With the cyclic volatility of the price of oil in the market and climate change, there is a pressing need to develop strategies for diversifying sources of energy for power generation and to promote the use of renewable energy to meet an ever increasing electrical demand.

Due to the effects of continuous and all year round trade winds, wind energy is a viable renewable energy source. Given that Mauritius is located among the Mascarene Islands, the transportation of wind turbine blades does increase its overall carbon footprint. Moreover, these blades are usually made up of fiberglass, carbon or Kevlar fibres which are derivatives of petroleum. In recent time, there has been a shift towards the production of wind turbine blades using natural fibres but the main problem plaguing this development is the lower mechanical strength provided by such fibre reinforced blades. On the other hand, there has been significant research in the use of Nano cellulose as reinforcing agent and they do boast better mechanical strength. Moreover UMaine Nanomaterial Pilot Plant has made the production of cellulose nanofiber from lignocellulosic fibres and wood on a large scale possible.

II. MATERIALS AND METHODS

A. Fibre characterisation

A group of Sansevieria Trifasciata (S.T) plants growing in a sun lit area near the banks of River Citron, Pamplemousses was selected from which healthy leaves were sampled. The leaves were hand washed under running water.

The fibres were extracted using a Phoenix decorticator whereby leaves of about 55 cm in length were fed into the fluted feed of the machine, then the continuous impact of the rotating drum of stripping blade remove the cuticle and epidermal layer of the leaf (Rafidison et al., 2018).

Manual extraction of the fibres were performed following by the process of water retting the fibres for two weeks to remove excess of plant matter remaining after the extraction process. The retted fibres were first rinsed by water for several minutes to remove the residual impurity then dried in an oven at 60^{o}C (Deesoruth et al., 2014; Abral et al., 2012) for 24 hours and stored in an air tight container to prevent moisture absorption (Rafidison et al., 2018).

The tensile tests of the 50 fibres were carried out prior to any post – extraction fibre refining process according to ASTM C1557 standard using a Testometric M500 – 50AT using a 10 kgf load cell and a gauge length of 25.4 mm (Wolela et al., 2019). The thickness of the fibre was measured against a dark background using a DigiMicro Profi 5MPix Microscope digital magnification 30x with a maximum resolution of 2592 x 1944, equipped with an image acquisition software. Five points were noted on a fibre using a marker and five thickness readings were noted at each point using an open sourced software as Image J software (Nadlene et al., 2015).

Pandanus Utilis (P.U) tree of the age of around two years old was selected from a sunlit area in the farm of the Curepipe Forestry Division whereby leaves of up to 2 m in length were sampled. Spiny and midribs of the leaves was removed using a knife and hand washed under running water (Abral et al., 2012). Similar extraction procedure and tensile tests were performed as per that of the Sansevieria Trifasciata fibre.

B. Yield determination of pre-extraction processing

The yield of fibre from a leaf is important from a commercial and environmental point of view. The higher the yield of extracted fibre from a leaf, the lower the number of leaves that need to be cut and hence lower environmental impacts associated with waste disposal after extraction processes. Regarding the commercial aspect, higher the yield of fibre will lower the initial investment for the cultivation of plants on large scale.

The fibre yield was calculated from the dry mass of a leaf at 60ºC for 24 hours in an oven. The mass of the combined dry fibre and waste was then dried off and weighed (Rafidison et al., 2018). The fibre field is calculated as per Equation (1):

Fibre yield= (mass of dry fibre)/(mass of dry fibre+waste) x 100% (1)

Given that yield values from the different methods listed above are close to each other the mechanical extraction was chosen based solely on the fact that fibres was already being extracted using similar process. This process was performed on five leaves from each biomass. The leaves chosen from each biomass were of equal length.

C. FTIR Tests

Fourier-Transform Infrared Spectroscopy (FTIR) Tests were performed for both samples: S.T and P.U fibres using a Bruker single bounce ATR-FTIR spectrometer equipped with OPUS software. This test is perform in order to determine the functional groups present in the fibre under analysis. The wavelengths that corresponds to a functional group will indicate its presence before and also its removal after a chemical treatment (B.H. Rafidison et al., 2018).

Crystallinity indices were also determined from the absorbance spectra by first applying baseline correction and the height of the peaks at the following wavelengths were determined (Ciolacu et al., 2011; Khai et al., 2017; Poletto et al., 2013).

The ratio between the absorbance heights of the peaks at 1371 cm^{-1} and 2901 cm^{-1} as defined by Ciolacu et al., 2011; Khai et al., 2017; Poletto et al., 2013, as the Total Crystalline Index (TCI) refers to the infrared crystallinity ratio.

Total Crystalline Index, TCI= A_1371/A_2901 (2)

The absorbance peaks at 1420 cm^{-1} is due to the amount of crystalline structure of cellulose and the peak at 893 cm^{-1} is associated with the amorphous region in the cellulose (Ciolacu et al., 2011; Khai et al., 2017; Poletto et al., 2013). The expression below is used to determine the Lateral Order Index (LOI):

Lateral Order Index, LOI= A_1420/A_893 (3)

The ratio of the absorbance peaks at 3350 cm^{-1} and 1318 cm^{-1} is used to determine the Hydrogen Bond Intensity of the cellulose samples (Ciolacu et al., 2011; Khai et al., 2017; Poletto et al., 2013)). The expression below is used to determine the Hydrogen Bond Intensity (HBI):

Hydrogen Bond Intensity, HBI=A_3350/A_1318 (4)

D. Isolation of cellulose nanocrystals

All glassware used was first washed thoroughly with distilled water and the same electronic weighing balance was used throughout the investigation.

The dried fibres were pulverized using a Fritsch Power Cutting Mill Pulverisette 15 and a sieve size of 1.0 mm. the intent of the process is to ensure grinding of the fibres and homogeneity in the sample size (Zafir et al., 2017).

1000 ml of 3 Wt. % of sodium hydroxide, NaOH solution was prepared by firstly measuring out 30g of NaOH pellets of 98% purity using a 3 d.p electronic balance. The NaOH pellets were dissolved in a small beaker of distilled water using a stirrer. Then the resulting solution was transferred to a 1000 cm^3 volumetric flask whereby it was top up to the mark using distilled water. The flask was then stoppered and shaken vigorously to obtain a homogenous solution. It was further poured in a 1500 ml beaker in which 50g of pulverized fibre was added. The mixture was stirred using a stirrer and was place on a hot plate set at 60ºC for 3 hours. The mixture was stirred at each 15 minutes mark.

After the required time has elapsed, the treated pulverized fibres was washed with distilled water until the pH became neutral and filtered using a filter paper. The pulp was then dried in an oven at 60ºC for 24 hours and the weight of the dried NaOH treated pulp was measured.

3 Wt. % of sodium hypochlorite, NaClO solution was prepared by diluting the available 12% solution by a factor of 4 through the addition of distilled water. The volume of 3 Wt. % of NaClO required corresponds to a solid to liquor ratio of 1:10. The NaOH treated pulverized fibres was then added to the solution and was allowed to reach a temperature of 60ºC on a hot plate for 3 hours. After the treatment time, white coloured pulps were observed.

A predetermined volume of 50 Wt. % of sulfuric acid was poured in a beaker under a fume hood. This volume corresponds to a solid/liquor ratio of 1:20. Using a hot plate set at 40ºC, the solution was heated first. Once the solution has reached the set temperature (measured with an alcohol in glass thermometer), the dried bleached pulp of S.T was carefully added. The mixture was allowed to hydrolyse for 30 minutes at 1000 rpm while maintaining a temperature of 40ºC. Approximately 1000 mL of distilled water was poured into the mixture to stop the reaction. Similar step were undertaken for dried P.U bleached pulp.

After the acid hydrolysis part, the solution was allowed to cool down to room temperature. For the centrifugation process, a centrifuge was required. As per the operating procedures of the centrifuge, balancing of each vials is extremely important as centrifugation depends of the principle of centrifugal forces. As a result of that, equal volume of

suspension was added to each vials. The suspension was poured in 16 vials and capped off and was placed in the dedicated slots in the centrifuge ring. The centrifuge lid was locked properly and the equipment was switched on.

This step was repeated twice to ensure an effective partial removal of sulfuric acid.

Only after the centrifuge equipment has given green light that proper balancing was done and no other error lights were seen, then 1500 rpm and 30 minutes was input and was set to start. The suspension was centrifuged at 1500 rpm for 30 minutes. After the time has elapsed, the vials look as shown below:

A clear difference could be seen between the fibrils and the remaining solution. The clear solution indicates that all the isolated Nano cellulose has successfully be separated from the suspension.

Afterwards, the solution was placed in dialysis tubing (Dialysis sacks Average flat width 25 mm, MWCO 12,000 Da from Sigma Aldrich) and was allowed to dialyzed against tap distil water until a neutral pH was reached (measured using a digital pH meter with distilled water as standard). The dialysis process took three to four days.

The suspension resulting from the dialysis was then sonicated (Q Sonic Sonicator) for 30 minutes with a pulse of 5 minutes to produce a stable Nano cellulose suspension. Pulse action was selected on the ultrasound generator as a safety precaution since the beaker containing the suspension was becoming hot which can eventually leads to explosion of the glassware. After sonication, the suspension was stored in an airtight container in a Laboratory refrigerator at 4ºC for later use.

75 mL of the Nano cellulose suspension was mixed with equal volume of ethanol and left in an air tight container for one day. The process of solvent exchange was carried out to remove the ethanol in the mixture. Hexane was then added to the remaining mixture and left in an air tight container for a day followed by solvent exchange. The set up for the solvent exchange make use of the Buchi Rotavapor R114 with the Buchi Waterbath B-480.

Firstly, the water bath was filled to the brim with water and the suspension containing the ethanol and Nano cellulose was filled in a round bottom flask which was then secured to the port as shown below. The whole apparatus was connected to a constant running of tap water to act as a cooling medium as per the standard operating procedures. As the boiling point of ethanol is around 78ºC, the water bath was set to similar temperature. The round bottom flask containing the suspension is set to a rotation motion to ensure overall and heating of the flask rather than on one spot only which can leads to fracture of the flask. The vacuum pump was turned on and all air taps was closed and the process was executed under vacuum.

Complete evaporation of ethanol was known when no more ethanol entered the empty round bottom flask. After all the ethanol has evaporated from the suspension, the water bath was switched off and the air tap was opened to create a point of air leakage else the cooling water will rushed into the empty round bottom flask. The latter was carefully removed and the ethanol was stored in an airtight container for later use.

The flask initially containing the suspension of Nano cellulose and ethanol, now had only the suspension of Nano cellulose. In the flask itself, hexane was added and the similar process was conducted but this time the temperature of the water bath is 68 ºC which is the boiling point of hexane.

The resulting mixture after complete evaporation of hexane, was then dried off in an oven for 24 hours at 40ºC. The dried Nano cellulose was stored in an airtight container at room temperature for later use.

E. Design of Experiments

According to Lee et al., 2014, the mechanical properties of CNC reinforced composites depend on the following factors: source of biomass, aspect ratio of CNC, orientation of CNC inside the matrix and amount of CNC content in the matrix. Given that investigation of variables such as aspect ratio of CNC, orientation of CNC is not possible in this current methodology as they require specialized equipment such as electrospinning, the other variables are going to be investigated.

According to Montgomery, 2013, given that there 2 factors being investigated, performing a one-factor at a time experiment is tedious as it will require lot of experimental runs. That is why full factorial experiment is being considered. Furthermore, as the number of observations for the latter is less, it also has a greater relative efficincy as compared to the one-factor at a time one.

Firstly, for the factor of source of biomass, two levels is being considered: S.T CNC and P.U CNC. As for the weight of CNC in the matrix, 0% to 5% (0 wt.% is the control of the experiment) is being considered as according to Alexandre and Dubois, 2000 and Borjesson and Westman, 2015, significant difference in the mechanical strength of CNC reinforced composites are noted. The following is the different experimental run at specific levels of both factors that need to be investigated as per Table 1.

TABLE I. DESIGN OF EXPERIMENT

Expt. No.	**Factors**	
	Type of CNC	**Wt.% of CNC in matrix**
1	S.T CNC	0%
2	S.T CNC	0.5%
3	S.T CNC	2.5%
4	S.T CNC	5.0%
5	P.U CNC	0%
6	P.U CNC	0.5%
7	P.U CNC	2.5%
8	P.U CNC	5.0%

ISSN No:-2456-2165

The tensile and flexural tests were performed in a Universal Testing Machine as per ASTM standards D638 and D790.

III. RESULTS

A. *Tensile test results for untreated S.T fibres and P.U fibres*

Table II below illustrates the tensile test results for untreated fibres.

TABLE II. TENSILE TEST RESULTS FOR FIBRES

	Untreated S.T fibre	Untreated P.U fibre
Sample Size	38	50
Mean/ MPa	370.504	124.710

B. *Fibre yield*

The fibre yield of S.T results are illustrated in table III as shown below:

TABLE III. FIBRE YIELD OF S.T

Leaf No.	Leaf 1	Leaf 2	Leaf 3	Leaf 4	Leaf 5
Fibre Yield/ %	16.9	15.0	16.1	16.3	17.1

A mean fibre yield percent of 16.3 was obtained.

The fibre yield of P.U fibre results are illustrated in table IV as shown below:

TABLE IV. FIBRE YIELD FOR P.U

Leaf No.	Leaf 1	Leaf 2	Leaf 3	Leaf 4	Leaf 5
Fibre Yield/ %	29.8	24.2	29.9	26.2	25.8

A mean fibre yield percent of 27.2 was obtained.

C. *FTIR results for S.T CNC and P.U CNC*

- *Comparison of spectra for untreated S.T fibre and S.T CNC*

The spectra for both the untreated S.T fibre and S.T CNC are shown in the figure 1.

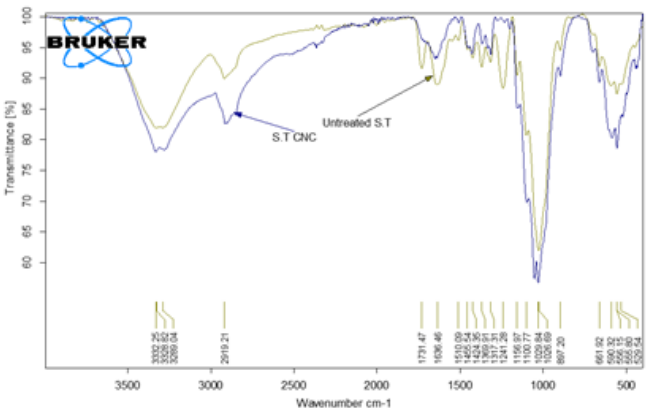

Fig. 1. FTIR for S.T

Considering the untreated S.T fibre, a strong absorption band in the region of 3400 to 3300 cm^{-1} was assigned to the O-H stretching vibration of the OH group in the cellulose molecules (Alexander & Dubois, 2000). In addition, a peak at 2919 cm^{-1} was mainly due to the C-H stretching vibration (Alexander & Dubois, 2000). Another peak at 1510 cm^{-1} attributes to aromatic skeletal vibrations of the benzene ring in lignin. The peak at 1241 cm^{-1} demonstrated the C-H bending of hemicellulose (Alexander & Dubois, 2000). The band at 1029 cm^{-1} corresponds to C-O / C-C stretching of the acetyl group in xylan (Hendriks A.T.W, 2009). A peak assigned at 1731 cm^{-1} is attributed to the C=O stretching vibration of the acetyl and uronic ester groups from pectin, hemicelluloses or the ester linkage of the carboxylic group of ferulic and p-coumaric acids of lignin and/or hemicellulose (Nadlene *et al*., 2015). Lignin was represented by peaks in the range of 1500-1600 cm^{-1} corresponding to the aromatic skeletal vibration (Abral *et al*., 2012). The peak at 1636 cm^{-1} represents the OH bending of the absorbed water (Alexander & Dubois, 2000). Similar peaks at 1424, 1369, 1317 cm^{-1} are associated with the bending vibrations of CH_2, C-H, and O-H groups of cellulose. The peaks observed at 897 cm^{-1} indicates the presence of the glucosidic linkages between the monosaccharides (Alexander & Dubois, 2000). The peak at 1731 cm^{-1} of hemicellulose is much lower in the case of the CNC which is a reflection of the removal of hemicellulose (Hao & Sheltami, 2018). This is mainly due to the removal of the carboxylic group by the alkali treatment performed by the process of deesterification. Similarly, the peaks at 1369 cm^{-1} and 1241 cm^{-1} indicate the presence of lignin and hemicellulose respectively. The peak at 1369 cm^{-1} is reduced in the case of the S.T CNC and that of 1241 cm^{-1} has nearly disappeared. This indicates that the hemicellulose was completely eliminated from the fibres than lignin after alkalization (Kamar *et al*., 2017). The range of wavelengths between 529 cm^{-1} and 661 cm^{-1} is much stronger in the CNC sample as compared to that of the fibre part. This is due to the C-Cl stretching present after the bleaching process (Joncas, 2010).

ISSN No:-2456-2165

➢ *Comparison of spectra for untreated P.U fibre and P.U CNC*

Similar observations could be made in this case. But differences were observed in the heights of the peaks when comparing S.T and P.U as illustrated in figure 2.

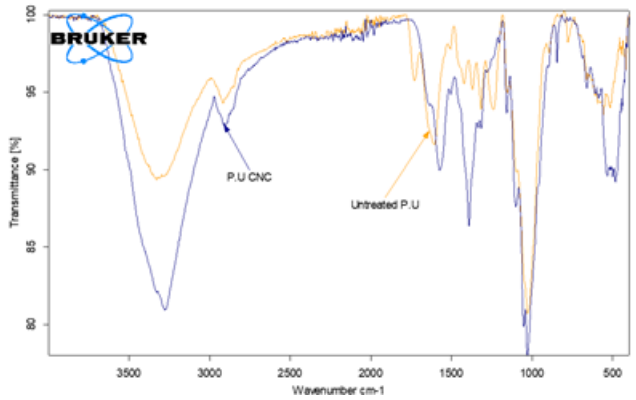

Fig. 2. FTIR for P.U

➢ *Crystallinity indices*

A lignocellulosic biomass constitutes mainly of hemicellulose, lignin and cellulose. Hemicellulose and lignin exists as amorphous structures but given the hydrogen bond present in the molecular structure of cellulose, it can exists in crystalline form. This implies that any changes in the morphological structure and composition of the latter can be analysed using the crystallinity of the fibres.

The FTIR spectra for both biomasses were analysed for the intensity of their peaks at 893, 1318, 1371, 1420, 2901 and 3350 cm-1. Using these values, the TCI, LOI and HBI indices were determined as illustrated in table V.

TABLE V. INDICES

Index	S.T	P.U
Untreated Fibres		
TCI	0.95	1.25
LOI	1.50	2.10
HBI	2.05	1.96
Isolated CNC		
TCI	0.38	2.03
LOI	0.56	1.80
HBI	3.75	2.73

TCI has a directly proportional to the crystallinity degree of cellulose and LOI is related to the overall degree of order in cellulose. Comparing the two untreated biomass, it is noted that the TCI of P.U is higher than that of S.T in order of 1.3 times and also the LOI of P.U is about 1.4 times higher than that of S.T. this implies that untreated P.U fibre has a higher degree of crystallinity and more ordered cellulose structure than untreated S.T fibre.

Comparing the TCI and LOI indices of the isolated CNC of each biomass, P.U CNC has higher TCI and LOI than S.T CNC by the order of 5.3 times and 3.2 times respectively. On the other hand, comparing the TCI and LOI between the untreated fibre and isolated CNC for each biomass, a decrease in both indices was noted for untreated S.T fibre and S.T CNC. Subsequently, an increase was noted in the TCI and a decrease in the LOI were recorded for untreated P.U fibre and P.U CNC.

Generally, after subsequent chemical treatment, an increase in the TCI should be noted. This is due to that fact that after a chemical treatment, non-cellulosic constituents and the amorphous regions are being removed and hence exposing the crystalline cellulose which results in higher TCI (Hendriks A.T.W, 2009). This statement holds true for the case of P.U biomass but not for S.T. One possible explanation for the case of S.T is that the sodium hydroxide solution penetrates the crystalline regions of cellulose to form soda celluloses. The possibility of the occurrence of random cleavage of cellulose in the chains of the crystalline domain. The crystallites can therefore cleave at random causing disorder in the fibre crystallites which need to be termed as amorphous as they are no more part of the crystalline structure (Ljungberg N *et al*., 2006).

As for the decrease in the LOI, this is due to mercerisation process (alkalisation process). Cellulose I is the cellulose synthase in the cell membrane of plant and they occur in parallel chains. Therefore there is an order structure observed in untreated plant fibres (Kamar *et al*., 2017). The alkali being used in this process infiltrates the cellulosic fibre and causes a rearrangement of the crystal packing of the chains of native cellulose I (chains are aligned in parallel) to cellulose II (chains are anti parallel) (Eichhorn SJ, 2011). Therefore a lower degree of order is noted which leads to decrease in the LOI after chemical treatment.

As for the HBI, considering the untreated fibres, their value of comparable to each other but for their respective CNC, S.T CNC has a higher value than P.U CNC in the order of 1.4 times. In all cases, a general increase in HBI was noted after chemical treatment. This due to the increase in cellulose chain mobility associated with the cellulose II as the anti-parallel chains enables the formation of inter-chain and inter-plane hydrogen bonds (Khai *et al*., 2017).

According to Hao & Sheltami, 2018, crystallinity of a fibre affects its tensile strength. The higher the crystallinity of the fibre, the fibre molecular arrangement in the slot holes are less and relatively small and a stronger bonding force between the molecules are observed.

ISSN No:-2456-2165

D. Tensile test results for CNC reinforced polyester composite

The tensile test results are illustrated in table VI.

TABLE VI. TENSILE TEST RESULTS

Wt. % of CNC in composite	0.0	0.5		2.5		5.0	
	Unreinforced Polyester	**S.T CNC**	**P.U CNC**	**S.T CNC**	**P.U CNC**	**S.T CNC**	**P.U CNC**
Sample mean/ MPa	9.563	20.200	12.92	25.817	18.47	30.500	22.98
Sample Standard deviation/ MPa	0.233	0.777	0.38	0.462	2.60	1.448	3.32

E. Flexural test results for CNC reinforced polyester composite

The flexural test results are illustrated in table VII.

TABLE VII. FLEXURAL TEST RESULTS

Wt. % of CNC in composite	0.0	0.5		2.5		5.0	
	Unreinforced Polyester	**S.T CNC**	**P.U CNC**	**S.T CNC**	**P.U CNC**	**S.T CNC**	**P.U CNC**
Sample mean/ MPa	13.579	21.491	19.530	33.417	21.490	41.587	28.30
Sample Standard deviation/ MPa	1.126	2.227	1.005	1.986	0.833	2.748	2.341

F. Discussion related to the tensile strength of untreated fibres

The main results regarding the tensile strength of the untreated fibres are their mean value and their respective standard deviations. The mean tensile strength of the S.T fibre was greater than that of P.U fibre.

One possible explanation for the difference in tensile strength of fibre is the use of TCI and LOI. As a greater value of TCI indicates the crystallinity degree of the cellulose. In general, a higher TCI will indicate a higher tensile strength. This is also supported by the LOI as greater the value of LOI, the more orderly arranged are the crystalline structure which are more compact and leads to a higher tensile strength of the fibre. But in this case the TCI and LOI of greater magnitudes were noted for the P.U fibre which does not corresponds to the tensile strength recorded.

Another explanation to support the tensile test results are the cellulose content. Cellulose provided the framework of the fibre structure whereby it provides strength, stiffness and structural stability of the fibre. This implies that a greater cellulose content, will indicate a larger tensile strength (Ciolacu et al., 2011). This is in conformance to the tensile test results obtained as the cellulose content for S.T fibre is 56% (Hendriks A.T.W, 2009) and that of P.U fibre is 30% (Abral et al., 2012). Moreover a greater correlation degree with respect to the tensile strength of fibre was noted for cellulose content as compared to that of the crystallinity index.

Secondly, a much greater standard deviation was noted in the tensile strength of S.T fibre as compared to that of P.U fibre. One possible explanation is based on the morphological properties of the fibre. According to (Fujii, 2017) , plant fibres differ in the morphological aspect due to factors such as internal area of lumens, number of lumens present, number and size of fibre cells, thickness of the secondary cell walls and the real cross sectional area of the fibre (given by the total area minus the lumen area). As the internal area of the lumens decrease (depends on the age of the plant: lumen internal area decrease as plant matures), the secondary cell wall thickens which causes an increase in the fibre strength (Fujii, 2017). Similar results were obtained by Nadlene et al., 2015, where roselle fibre at 3 months old had a tensile strength of 405 MPa and that of 9 months old was 207 MPa. The higher standard deviations noted for S.T fibre is related to the sourcing of the biomass whereby the leaves were cut from different plants (the plant age may vary greatly) from the same area as compared to the P.U leaves which all were from a single plant.

G. Discussion related to the tensile and flexural strength of CNC reinforced composite

Two main conclusions were drawn from the results of the tensile and flexural tests. Firstly a general increase in strength was noted as Wt. % of CNC in the polyester increases for both biomass. Secondly, at any Wt. % of CNC, the respective tensile or flexural strength of S.T CNC reinforced composites were higher than that of P.U ones.

Firstly, concerning the difference in strength of between the two CNCs, as it was in the previous section that cellulose content of a fibre is responsible for the tensile strength of the fibre. Similarly, a higher concentration of cellulose in the fibre will lead to the lowest ratio length to diameter (also known as L/d ratio or the aspect ratio) (Elazzouzi S, 2006). Since the actual aspect ratio of the isolated CNCs for both biomass could be measured due to agglomeration (this was possibly due to formation of hydrogen bonds between the nanocrystals during the drying process), the former statement will be considered to hold true in this case (Elazzouzi S, 2006). This implies that S.T CNC will have lower aspect ratio as compared to that of P.U CNC.

The aspect ratio of CNC is dependent on the percolation threshold (φFc) of the nanocrystals (Elazzouzi S, 2006). Given that S.T CNC has lower aspect ratio as compared to that of P.U CNC, this implies that, S.T CNC will have higher percolation threshold as compared to P.U CNC. According to Elazzouzi S, 2006, if the weight fraction of the reinforcement in the polymer is higher than the percolation threshold, then the density of the cellulose nanocrystals in the matrix is adequate to allow the connection of the nanocrystals through hydrogen bonding to produce a continuous three dimensional network in the composite (Elazzouzi S, 2006). This is relevant in cases where the Nano filler was random and the composites were produced through casting.

One possible explanation for the higher strengths for S.T CNC reinforced composites is that the difference between its percolation threshold and the different weights percent of CNC investigated is much higher than that of P.U CNC reinforced composites. Therefore, the three dimensional network created inside the matrix using S.T CNC is more extensive as compared to that of P.U CNC reinforced polymer. Moreover this is supported by the higher HBI of S.T CNC as compared to that of P.U CNC resulting in the S.T chains of cellulose molecules having a greater chain mobility than that of P.U chains. As reinforcement in the matrix, a greater chain mobility will result in higher inter-chain and inter-plane hydrogen bonding, hence contributing to a much higher strength.

Secondly, concerning the general increase in strength with an increase in wt. % of CNC in matrix for both biomass, this is due to the fact as the weight percent of CNC is being increased, there is much larger surface area of nanocrystals which are in contact with the matrix (Mendes et al., 2015). Hence resulting in a greater amount of hydrogen bonding is possible between the nanocrystals and the matrix. Also better interaction between the matrix and nanocrystals will result in a better stress transfer between thee matrix and the filler leading to greater strengths as weight percent of CNC in matrix is increased.

IV. CONCLUSION

A solution using wind turbine blade was proposed based on the problem described. CNC from *Sansevieria Trifasciata* and *Pandanus Utilis* were chosen as reinforcement for polyester based composites. The investigation carried out determined a maximum tensile and flexural strength at 5 Wt.% of CNC. The observations made during this project have all been related to Literature. To conclude, the use of local biomass as reinforcement in wind turbine blade is feasible in Mauritius and for the use case in Mauritius.

REFERENCES

[1]. Abody, R. C. N. A. L., 2016. Nanocellulose, a tiny fibre with nugh applications.
[2]. Abral, H. et al., 2012. Mechanical properties of screw pine(Pandanus Odoratissimus) fibers unsaturated polyester composites.
[3]. Alexander, M. & Dubois, P., 2000. Polymer layerd silicate nanocomposites: preparation, properties and uses of a new class of materials.
[4]. Angles MN, D. A. & Dufresne, A., 2000. Plasticized starch/tunicin whiskers nanocomposites..
[5]. Ashwill, T., 2009. Materials an innovations for Large blade structures.
[6]. Bonini C, H. L. C. J.-Y., 2000. Polypropylene reinforced with cellulose whiskers.
[7]. Borjesson, M. & Westman, G., 2015. Crystalline Nanocellulose-Preparation, Modification and properties.
[8]. Brinchi, L., Cotana, F., Fortunati, E. & Kenny , J., 2013. Production of nanocrystalline cellulose from lignocellulosic biomass.
[9]. Castaneda-Garza, G., Valerio-Urena, G. & Izumi, T., 2019. Visual Narrative of the Loss of Energy after natural disasters.
[10]. Chauve G, H. L. A. R. M. K., 2005. Cellulose poly(ethylene-co-vinyl acetate) nanocomposites studied by molecular modeling and mechanical spectroscopy.
[11]. Ciolacu, D., Ciolacu, F. & Popa, V., 2011. Amorphous cellulose-structure and characterization.
[12]. Deesoruth, A., Ramasawmy, H. & Chummun, J., 2014. Investigation into the use of alkali treatedscrewpine (Pandanus Utilis) fibres as reinforcementin epoxy matrix.
[13]. Deshpande K., G. H. G. H., 2014. Extraction of cellulose by CMt techniques.
[14]. Dufresne, 2000. Dynamic mechanical analysis of the interphase in bacterial polyester/cellulose whiskers natural composites.
[15]. Dufresne, 2001. Interfacial phenomena in nanocomposites based on polysaccharide nanocrystals.
[16]. Eichhorn SJ, Y. R., 2011. Composite micromechanics of hemp fibres and epoxy resin microdroplets.
[17]. Ekundayp, G. & Adejuyigbe, S., 2019. Reviewing the development of natural fibre polymer composite.
[18]. Elazzouzi S, N. Y. P. J.-L. P. I. S. M., 2006. Chiral nematic suspensions of cellulose whiskers in water and in organic solvents.
[19]. Espimoza-Acosta, T. C. C. E. R. B., 2014. Ionic Liquids and solvents for recovering lignin from lignocellulosic biomass.
[20]. Fecko, D., 2006. High strength glass reinforcements still being discovered, Reinforced Plastics.
[21]. Fujii, 2017. Investigation of mechanical strength of microfibre reinforced PLA.
[22]. Grande, J., 2008. Wind Power Blades Energize Composites Manufacturing.
[23]. Haberkern, H., 2006. Tailor-made reinforcements, Reinforced Plastics.
[24]. Habibi Y, L. L. R. O., 2010. Cellulose nanocrystals: chemistry, self-assembly, and applications.
[25]. Hao, L. & Sheltami, R., 2018. Natural fibre reinforced Vinyl Ester and Vinyl polymer Composites.
[26]. Hendriks A.T.W, Z. G., 2009. Pretreatments to enhance the difestibility of lignocellulosic biomass.
[27]. Holmes, J. et al., 2009. Development of Bamboo-based composite as a Sustainable Green Material for wind turbine blades.
[28]. Holmes, J., Sorensen, B. & Brondsted, P., 2007. An overview of Materials Testing Wind Power.
[29]. Johnson, D. & Gu, M., 2016. Wind Turbine Performance in Controlled Conditions: BEM Modeling and Comparison with Experimental Results.
[30]. Joncas, S., 2010. Thermoplastic composite wind turbine blades: an integrated design approach.
[31]. Kalagi, G., Patil, R. & Nayak, N., 2016. Natural Fiber Reinforced Polymer Composite. *IJSDR*, Issue 2455-2631, p. 10.
[32]. Kamar, M., Adel, A. & El-Shafei, A., 2017. Influence of Cellulose Polymorphism on Tunable Mechanical and Barrier Properties of Chitosan/Oxidized Nanocellulose Bio-Composites.

[33]. Karthikeyan, N., Anand, R., Suthakar & Barhate, S., 2018. Materials, Innovations and Future Research Opportunities on Wind Turbine Blades.
[34]. Khai, D., Nhan, P. & Hoanh, T., 2017. An investigation of the structural characteristics of modified cellulose from acacia pulp.
[35]. Kim, S., Song, Y. & Hwang, T. Y., 2019. Facial fabrication of an inorganic/organic thermoelectric nanocomposite based gas sensor for hydrogen detection with wide range and reliability. Issue 10.1016/j.ijhydene.2019.03.004.
[36]. Kiziltas A, G. D. H. Y. Y. H.-S., 2011. Thermal properties of microcrystalline cellulose-filled PET-PTT blend polymer composites.
[37]. Lee, K., Hamid, S. & Zain, S., 2014. Conversion of Lignocellulosic Biomass to Nanocellulose.
[38]. Ljungberg N, Cavaille JY & Heux L, 2006. Nanocomposites of isotactic polypropylene reinforced with rod-like cellulose whiskers.
[39]. Ljungberg, N. et al., 2005. New nanocomposite materials reinforced with cellulose whiskers in atactic polypropylene.
[40]. Lystrup, A. et al., 1998. Hybrid yard for thermoplastic fibre composites.
[41]. Mendes, C., Ferreira, N., Furtado & de Sousa, A., 2015. Isolation and characterisation of nanoceystalline cellulose from corn husk.
[42]. Mishnaevsky, L. J., 2011. Composite materials in wind energy technology.
[43]. Mitrovic, C. & Vorotovic, G., 2014. ADVANCED STRUCTURAL TESTING METHODS FOR SMALL WIND TURBINES BLADE UP TO FAILURE.
[44]. Modenbach, 2013. Sodium Hydroxide pretreatment of corn stover and subsequent enzymatic hydrolysis.
[45]. Montgomery, D., 2013. *Design and Analysis of Experiments*. 8th ed. s.l.:John Wiley & Sons Inc.
[46]. Nadlene, R. et al., 2015. Material Characterization of Roselle Fibre as potential reinforcement material for polymer composites.
[47]. Nijssen, R., 2007. Fatigue Life prdiction and strength degradation of wind turbine rotor blade composites.
[48]. Noryani, M. et al., 2019. *Material selection of natural fibre using a stepwise regression model with error analysis.*
[49]. Okubo, 2016. Extraction of cellulose microfibres.
[50]. Ong, C. & Tsai, S., 2000. The use of Carbon fibres in wind turbine blade design.
[51]. Perrera B., A. V., 2018. Nanocelluloses from sugarcane biomass.
[52]. Poleto, M. & Pistor, V., 2013. Structural Chracteristics and Thermal properties of native cellulose.
[53]. Rafidison, B. H., 2019. *Composite material: An investigation into the use of Pandanus fibres for a small-scale wind-turbine blade application*, Mauritius: s.n.
[54]. Rafidison, B. H., Ramasawmy, H., Chummun, J. & Florens, F. B. V., 2018. Tree Age, Leaf Maturity and Exposure to Sunlight. *Journal of Natural Fibres*, p. 12.
[55]. Rajan T, G. H. A. R., 2015. Extraction of nanocellulose using chemical method.
[56]. Raut, S., Shrivas, S., Sanas, R. & Sinnarkar, N., 2017. Simulation of Micro Wind Turbine Blade in QBlade.
[57]. Sair, S., Oushabi, A., Kammouni, A. & Abdeslam, E. B., 2017. Effect of surface modification on morphological, mechanical and thermal conductivity of hemp fiber: Characterization of the interface of hemp –Polyurethane composite. Issue 10.1016/j.csite.2017.10.012.
[58]. Samir MASA, A. F. S. J.-Y. D. A., 2004. Cellulose nanocrystals reinforced poly(oxyethylene).
[59]. Santos, S., Carbajo, J. M. & Gomez, N., 2017. Modification of Bacterial Cellulose Biofilms with Xylan Polyelectrolytes. Issue 10.3390/bioengineering4040093.
[60]. Shah, D., 2014. Natural fibre composites: Comprehensive Ashby-type materials selection charts.
[61]. Shah, D., Schubel, P. & Clifford, M., 2013. *Can Flax replace E-glass in structural composites?*.
[62]. Yamashitra, 2018. Charaterisation of cellulose microfibre reinforced PLA.